Journal of Photochemistry & Photobiology A: Chemistry 364 (2018) 750–757

Contents lists available at ScienceDirect

Journal of Photochemistry & Photobiology A: Chemistry

journal homepage: www.elsevier.com/locate/jphotochem

A hydroxyphenylquinazolinone-based fluorescent probe for turn-on detection of cysteine with a large Stokes shift and its application in living cells

Huace Sheng[a], Yonghong Hu[a,b], Yi Zhou[c], Shimin Fan[b], Yang Cao[d], Xinxin Zhao[a], Wenge Yang[a,*]

[a] School of Pharmaceutical Sciences, Nanjing Tech University, No. 30, South Puzhu Road, Nanjing 211816, China
[b] The Synergetic Innovation Center for Advanced Materials, Nanjing Tech University, No. 30, South Puzhu Road, Nanjing 211816, China
[c] College of Chemistry and Molecular Engineering, Nanjing Tech University, Nanjing 211816, PR China
[d] Jiangsu Province Hospital, Nanjing 210000, China

ARTICLE INFO

Keywords:
Fluorescent probe
Cysteine
Aggregation-induced emission
Conjugate addition
Cell imaging

ABSTRACT

A hydroxyphenylquinazolinone-based fluorescent probe DAP-1 with a large Stokes shift (162 nm) was firstly developed for detection of cysteine. The probe DAP-1 with two acrylate as highly Cys-selective sites was designed based on the combination of excited state intramolecular proton transfer (ESIPT) and aggregation-induced emission (AIE) mechanism. Upon the treatment with cysteine, DAP-1 displayed a strong fluorescence enhancement (65-fold). The limit of detection obtained from fluorescent titration was as low as 0.03 μM. DAP-1 could detect cysteine with high selectivity and sensitivity. Significantly, DAP-1 could be used to detect cysteine in living cells.

1. Introduction

Biothiols, such as cysteine (Cys), homocysteine (Hcy) and glutathione (GSH), play crucial roles in protein synthesis, in maintaining biological redox homeostasis, and in post-translational control [1–3]. Normal levels of Cys (30–200 μM) maintain the synthesis of various proteins and act as the source of sulfide in human metabolism [4]. However, abnormal levels of Cys could result in certain diseases including liver damage, slow growth in children and Alzheimer's disease [5,6]. Hence, it is important to track Cys in living system.

Many techniques including, high-performance liquid chromatography [7], electrochemical methods [8], fluorescent probes [9–17], and mass spectroscopy [18] have been developed for the detections of bio-thiols. Among these detection techniques, fluorescent techniques are widely utilized in bio-thiol detection owing to its low detection limit and high sensitivity [11,10–17]. A lot of fluorescent probes based on different sensing mechanisms, including non-emissive Cu(II) complexes [19–22], cleavage reaction [12,23,24], cyclization reaction [25], Michael addition [26] and others [27] have been developed to detect biothiols. Nevertheless, discriminating Cys, GSH and Hcy (Scheme 1) is still challenging due to their structural similarity [28–30]. In the distinguishing Cys from Hcy and GSH, the conjugate addition/cyclization of Cys to acrylate group has demonstrated to be a valid method [31], which has been widely used in conventional chromophores including coumarin [30,32], 2-(2-hydroxyphenyl)quinazolin-4(3 H)-one (HPQ) [33,34], cyanine [35,36], benzothiazole [37,38], naphthalimide [39]. Unlike traditional chromophores suffering from fluorescence quenching in high concentration due to π-π interaction [40–46], aggregation-induced emission (AIE) chromophores such as HPQ and its derivatives are almost non-emissive when molecularly dispersed but become highly emissive in the aggregate state with fluorescence increasing along with the increase of chromophores concentration [47,48]. The AIE probes offer significant advantages of a high signal-to-noise ratio and excellent photostability [49,50].

Continuing on our research in this direction, we have developed a new double acrylate-functionalized fluorescent probe DAP-1 (Scheme 1) for detecting Cys. DAP-1 is derived from HPQ chromophore (compound 2) with two acrylate groups based on addition-cyclization reaction mechanism. Compound 2 displays a large Stokes shift (162 nm). It is known that chromophores with large Stokes shifts are more suitable for the application because they can greatly improve the detection sensitivity by reducing self-quenching and auto-fluorescence caused by the minimal overlap of excitation and emission spectra [51–55]. The acrylate group is commonly used as a functional trigger group to sense Cys [31,56,57], where the reaction with Cys generally exhibited faster reaction kinetics than GSH and Hcy [58–60]. Especially, double

* Corresponding author.
E-mail address: wengeyang11@163.com (W. Yang).

https://doi.org/10.1016/j.jphotochem.2018.07.014
Received 19 May 2018; Received in revised form 30 June 2018; Accepted 12 July 2018

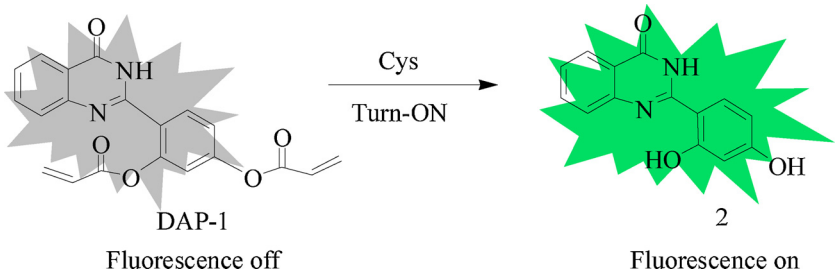

Scheme 1. Rational design of DAP-1.

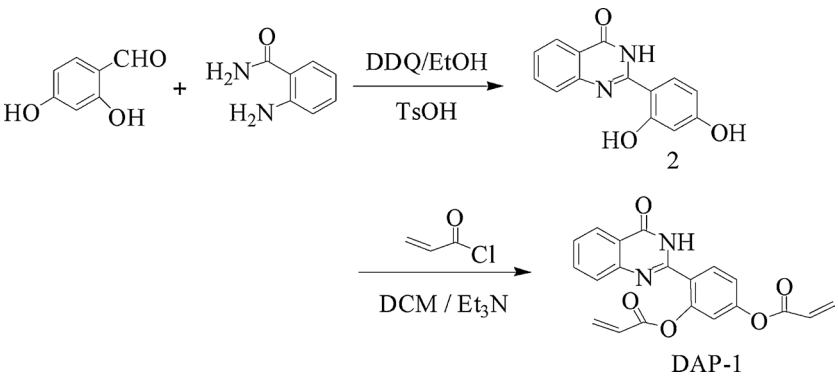

Scheme 2. Synthesis route of DAP-1.

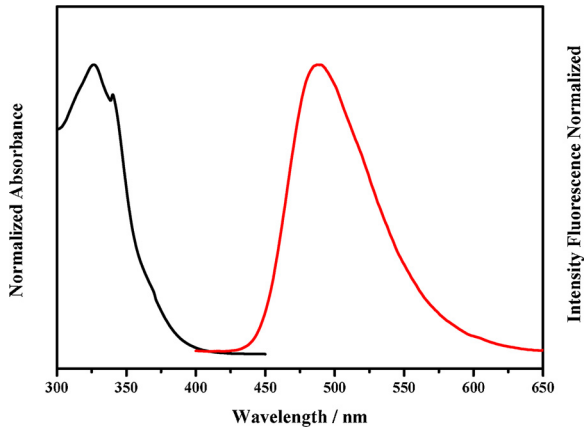

Fig. 1. Normalized absorption (black line) and fluorescence spectra (red line) of compound 2 in PBS/DMSO system (99/1, v/v, pH 7.4). (For interpretation of the references to colour in this figure legend, the reader is referred to the web version of this article.)

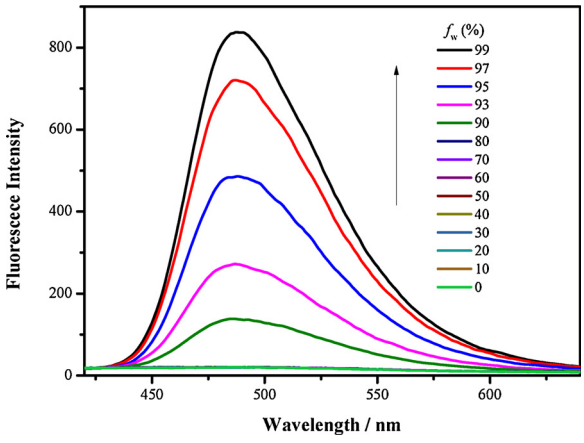

Fig. 2. Fluorescent spectra of compound 2 (10 μM) in water-DMSO mixtures with different fractions of water (f_w).

acrylate-functionalized probe DAP-1 can make the distinction of the reaction kinetics with bio-thiols even more evident, thus offering DAP-1 to actualize high sensitivity and selectivity for Cys over GSH and Hcy. To the best of our knowledge, DAP-1 is the firstly use of AIE chromophore HPQ with two acrylate groups to detect Cys. This probe DAP-1 has the following advantages: (1) it can be easily synthesized with good yield; (2) it displays a large Stokes shift; (3) it exhibits high signal-to-noise ratio and excellent photostability. The experiment results showed that DAP-1 could detect Cys with significant and rapid fluormetric response. Moreover, DAP-1 could be conveniently used in living cells imaging.

2. Experimental

2.1. Materials and instruments

All purchased chemicals and reagents are of analytic grade. ^{1}H NMR

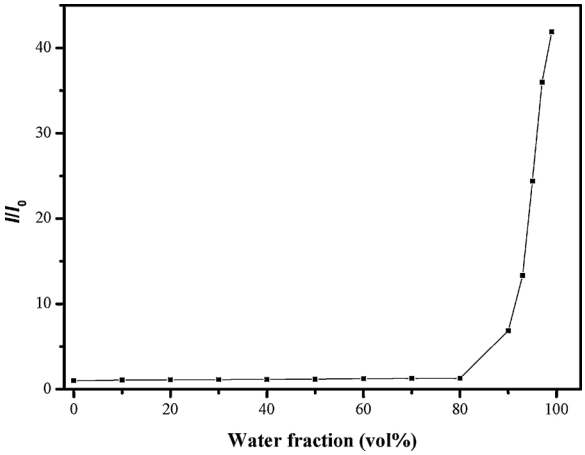

Fig. 3. Plot of relative fluorescent intensity (I/I_0) at 495 nm versus the solvent composition of the water -DMSO mixture of compound 2.

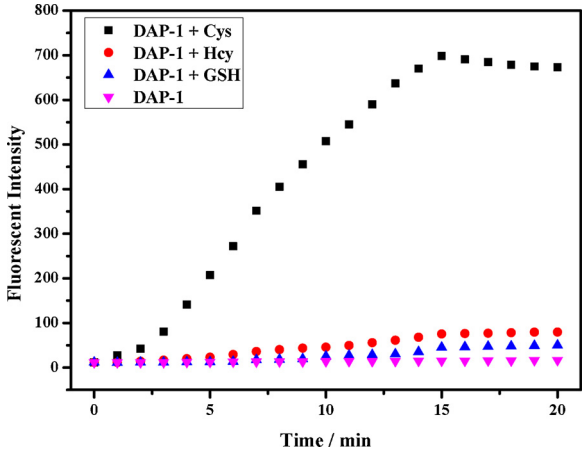

Fig. 4. Time-dependent fluorescence intensity at 495 nm of free DAP-1(10 μM) (pink) and DAP-1 with 10 equiv. of Cys (black), Hcy (red), and GSH (blue) in PBS/DMSO system (1/1, v/v, pH 7.4). (For interpretation of the references to colour in this figure legend, the reader is referred to the web version of this article.)

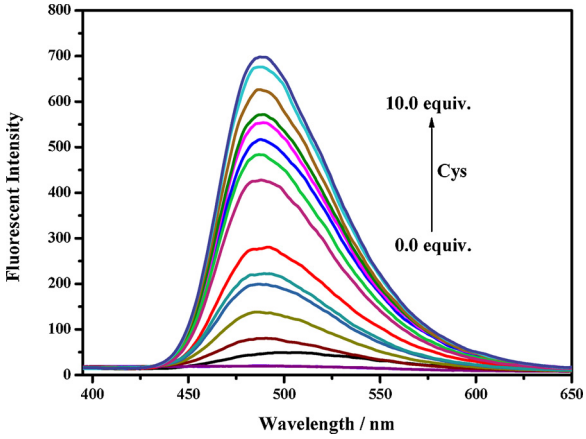

Fig. 5. Fluorescence spectra of 10 μM DAP-1 upon addition of 0–100 μM Cys in PBS/DMSO system (1/1, v/v, pH 7.4). λ_{ex} = 333 nm, slit width: d_{ex} = d_{em} = 5 nm.

and ^{13}C NMR were measured on AVANCE III400MHz Digital NMR Spectrometers (Bruker Daltonics Corp., USA), using tetetramethylsilane (TMS) as an internal reference. Electrospray ionization mass spectra (ESI-MS) were measured on a Micromass LCTTM system. Fluorescence spectrum was recorded on a spectrofluorimeter (Shimadzu RF-5301PC) equipped with 1.0 cm quartz cell.

2.2. General procedure for spectral measurements

Stock solution of DAP-1 (10 mM) and N-ethylmaleimide (NEM, 100 mM) were prepared in DMSO. Stock solutions of 10 mM Cys, GSH, Glu, Thr, Ser, Ala, Asp, Phe, Val, Leu, His, Trp, IIe, Hcy, Arg, Lys were prepared by direct dissolution in deionized water. All the detection experiments were measured in PBS buffer-DMSO (1:1, v/v, pH = 7.4). The procedure was as follows: into a PBS buffer-DMSO (1:1, v/v, pH = 7.4) solution, containing 10 μM probe DAP-1, an analyte sample was added. The process was monitored by fluorescence spectrometer.

2.3. Synthesis of compound 2

2-Aminobenzamide (680.8 mg, 5 mmol) was dissolved in anhydrous EtOH and followed by the addition of 2,4-Dihydroxybenzaldehyde (690.6 mg, 5 mmol). The reaction was refluxed in the presence of TsOH (p-Toluenesulfonic acid, 0.02 g, 0.1 mmol) for 90 min. The resulting solution mixture was cooled to 0℃, and DDQ (2,3-dichloro-5,6-dicyano-4-benzoquinone, 1.14 g, 5 mmol) was added. The mixture was slowly brought to room temperature for another 60 min and a reddish brown solid was formed. The solid was collected by filtration and washed with a small amount of cooled ethanol, which was further purified by recrystallization using ethanol to afford the desired pale yellow compound 2 (1.09 g, 85% yield). ^{1}H NMR (400 MHz, DMSO-d_6) δ 14.25 (s, 1 H), 12.28 (s, 1 H), 10.31 (s, 1 H), 8.11 (d, J = 7.8 Hz, 2 H), 7.81 (t, J = 7.2 Hz, 1 H), 7.66 (d, J = 7.9 Hz, 1 H), 7.47 (t, J = 7.2 Hz, 1 H), 6.48 – 6.28 (m, 2 H). ESI-MS: calcd for $C_{14}H_{12}N_2O_3$ $[M+H]^+$ 255.1, found 255.1.

2.4. Synthesis of DAP-1

Compound 2 (381.3 mg, 1.5 mmol) was dissolved in dry dichloromethane (15 mL) And then acryloyl chloride (271.5 mg, 3 mmol) and triethylamine (420 μL, 3 mmol) were sequentially added. The mixture was stirred for 1 h at 25 ℃. Next, 15 ml H_2O was introduced into the mixture. The resulting solution was extracted with CH_2Cl_2 (15 mL × 3) and dried over anhydrous Na_2SO_4. The solvent was concentrated under Rotavapor. The residue was purified by column chromatography using petroleum ether /ethyl acetate (5:1) to give DAP-1 as a white solid (407.3 mg, 75% yield). ^{1}H NMR (400 MHz, DMSO-d_6) δ 8.15 (d, J = 7.7 Hz, 1 H), 7.90 (d, J = 8.4 Hz, 1 H), 7.82 (t, J = 7.5 Hz, 1 H), 7.62 – 7.50 (m, 2 H), 7.42 – 7.30 (m, 2 H), 6.60 (d, J = 17.2 Hz, 1 H), 6.47 (td, J = 17.1, 12.4 Hz, 2 H), 6.31 (dd, J = 17.2, 10.4 Hz, 1 H), 6.21 (d, J = 10.3 Hz, 1 H), 6.10 (d, J = 10.5 Hz, 1 H). ^{13}C NMR (101 MHz, DMSO-d_6) δ (ppm) 164.18, 163.90, 162.19, 152.61, 150.64, 149.29, 148.92, 135.01, 134.77, 134.44, 131.88, 127.84, 127.79, 127.76, 127.38, 126.25, 125.06, 121.43, 120.14, 117.82. HR-MS: calcd for $C_{20}H_{16}N_2O_5$, $[M+H]^+$ 363.0903, found 363.1011.

Detailed procedures were described in Scheme 2 and characterizations were shown in supporting information (Fig. S1-S5).

2.5. Confocal fluorescence imaging and Cytotoxicity assay

HeLa cells were cultured in Dulbecco's Modified Eagle's Medium (DMEM) supplemented with 10% fetal brovine serum, 100 μg/mL penicillin and 100 μg/mL streptomycin at 37 ℃ in a humidified atmosphere containing 5% CO_2. To imagine endogenous Cys, HeLa cells were only treated with DAP-1 (10 μM). In another experiment group, HeLa cells were first incubated with N-methylmaleimide (NEM, a thiol-blocking reagent) and then treated with DAP-1. For imaging exogenous Cys, HeLa cells were first pre-incubated with NEM and Cys. Then DAP-1 were added to the cells. MTT assay was further conducted to investigate the cytotoxicity of DAP-1. Before the treatment of cells with DAP-1, HeLa cells were plated in 96-well plates and incubated in growth medium for 24 h. Next, HeLa cells were co-incubated with different concentration of DAP-1 (0, 10, 20, 50 and 100 μM) at 37 ℃ for 24 h. Finally, MTT reagent were added at 37 ℃ for 4 h.

3. Results and discussion

3.1. Probe design and synthesis

DAP-1 was designed using compound 2 as the chromophore and two acrylate groups as the recognition sites. Compound 2 is a typical AIE chromophore due to excited state intramolecular proton transfer (ESIPT) and restriction of intramolecular motion (RIM) [33,34]. We first investigated the absorption and emission spectrum of compound 2 (Fig. 1). As shown in Fig. 1, compound 2 is markedly fluorescent (Φ = 0.225) with a maximum at 495 nm (λ_{Abs} = 333 nm) and a lager Stokes shift (162 nm). It is well known that chromophores with lager Stokes shifts could improve the detection sensitivity by reducing the overlap of excitation and emission bands [51–53], which are much

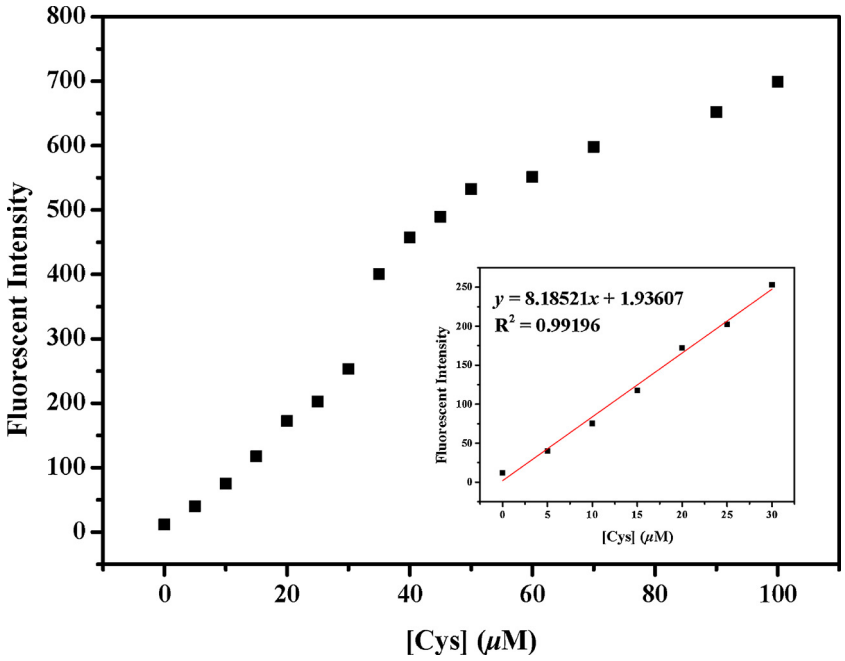

Fig. 6. The plot of fluorescence intensity at 495 nm versus the concentration of Cys. Inset: the linear relationship between the fluorescence intensity and Cys concentration (0–30 μM).

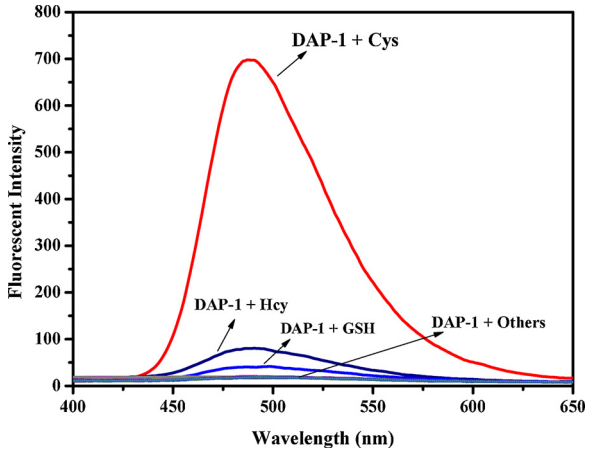

Fig. 7. Fluorescence spectra of DAP-1 (10 μM) after treated with various 100 μM amino acids (Cys, GSH, Glu, Thr, Ser, Ala, Asp, Phe, Val, Leu, His, Trp, IIe, Hcy, Arg, Lys) in PBS/DMSO system (99/1, v/v, pH 7.4).

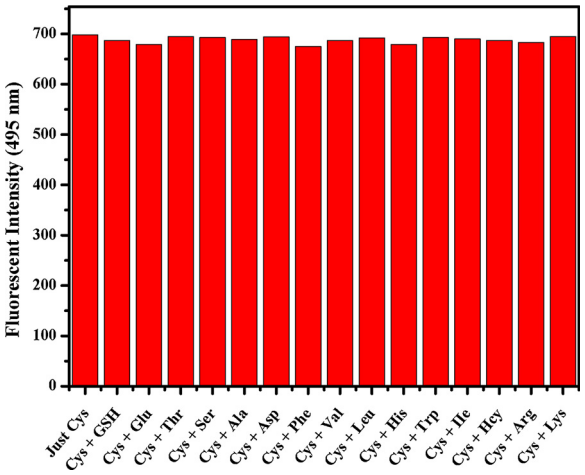

Fig. 8. Fluorescent response of DAP-1 (10 μM)at 495 nm toward Cys (100 μM) in the presence of various analytes (1 mM).

desirable for in vivo application. Hence, we chose the compound 2 as the chromophore to construct probe DAP-1. As mentioned above, acrylate group has been proved to be effective recognition and quenching group for sensing Cys. Hence, we introduced two acrylate groups to the compound 2, thus offering the double acrylate-functionalized probe DAP-1 (Scheme 1). As shown in Scheme 1, the fluorescence of DAP-1 was efficiently quenched due to blocking the intramolecular hydrogen bond and free rotation of the C—C bond. Once the DAP-1 reacts with Cys, the fluorescence of corresponding product (compound 2) would quickly recover to the 'On-state' through intramolecular hydrogen bond formation to trigger the ESIPT process and aggregation in aqueous media to trigger the AIE process. Based on the above principles, a simple probe DAP-1 with 'Off-On' fluorescence response to Cys was designed. We also investigated the photostability of DAP-1 using time-based fluorescence spectroscopy (Fig. S6). As shown in Fig. S6, the fluorescence intensity of DAP-1 showed almost no change over a course of 360 min, while the fluorescence intensity of fluorescein, a well-known organic dye, decreased gradually under the same condition. The result indicates that DAP-1 displays a good photostability. Other photophysical properties of DAP-1 are presented in Table S1. Synthesis of DAP-1 is outlined in Scheme 2. First, compound 2 was synthesized by the reaction of 2-Aminobenzamide and 2,4-Dihydroxybenzaldehyde. Next, DAP-1 was readily synthesized by the acylation reaction from compound 2 and acryloyl chloride. The ^{1}H NMR, ^{13}C NMR and HR-MS of DAP-1 and compound 2 were shown in Fig. S1-S5.

3.2. AIE properties of compound 2

As mentioned above, DAP-1 is almost non-emissive when molecularly dispersed (Scheme 1). However, DAP-1 could react with Cys to generate AIE chromophore compound 2, which could become highly emissive in the aggregate state. We assumed that the detection of Cys was mainly completed by measuring the fluorescence intensity that attribute to the formation of compound 2. Hence, we first investigated the AIE properties of compound 2 by measuring its fluorescent spectra in H_2O/DMSO mixtures with different water fractions (Fig. 2). As is

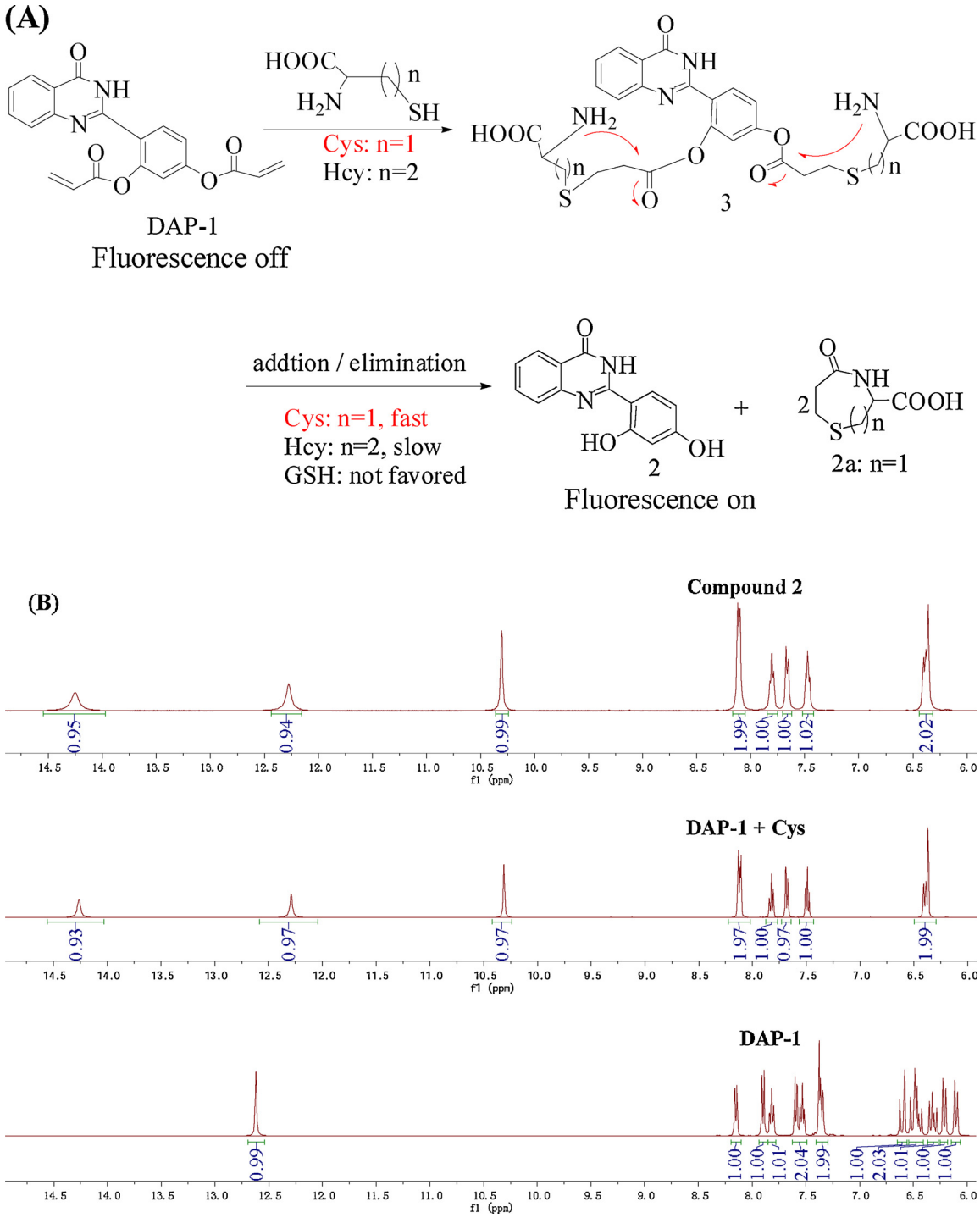

Scheme 3. (A): The proposed reaction mechanism of DAP-1 and Cys. (B): ^{1}H NMR spectra of Compound 2, DAP-1-Cys reaction products and DAP-1.

shown in Fig. 2, compound 2 (10 μM) is almost non emissive in pure DMSO solution. The solubility of compound 2 can be reduced by the increasing water fractions in H_2O/DMSO mixture and induce the formation of nanoaggregates. Although the fluorescence intensity of compound 2 remained low with water contents ranging from 0 to 90 vol %, it increased rapidly when the water contents increase from 90 to 99 vol %. At the 99 vol % water fractions, the fluorescent intensity is about 42-fold than that in the pure DMSO solution (Fig. 3). This phenomenon indicates that compound 2 is AIE-active and the ESIPT process can smoothly proceed in aggregation state by avoiding the disrupting on intromolecular hydrogen bond from polar solvents. We selected this optimized H_2O/DMSO (99:1, pH 7.4) solution for the subsequent fluorescence measurements.

3.3. Kinetic studies

To get the optimal reaction time, a time-dependent fluorescence intensity measurement was conducted on DAP-1 (10 μM) with 10 equivalent Cys, GSH and Hcy at pH 7.4. As we can see from Fig. 4, the fluorescence intensity increases instantaneously and reaches a plateau at around 15 min when Cys (100 μM) was added to the solution of DAP-1. As for Hcy and GSH, the fluorescence intensity changed very weakly. In addition, the fluorescence intensity of DAP-1 without above biothiols was negligible during the same reaction time. We also evaluated the

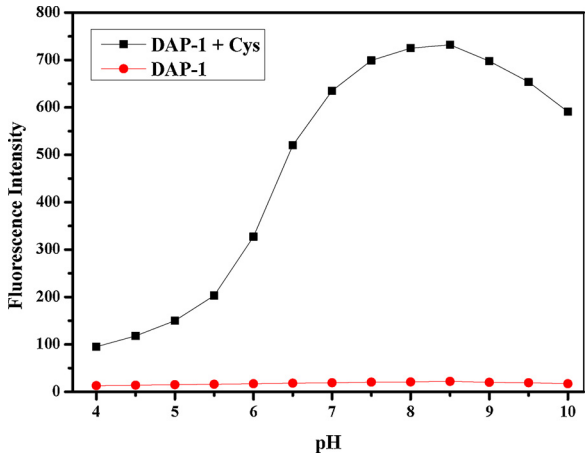

Fig. 9. Fluorescence intensity of DAP-1 (10 μM) in the absence and presence of Cys (100 μM) at 495 nm at various pH values.

time-dependent emission enhancement of DAP-1 at pH 8.0 and 8.5. As shown in Fig. S7 and S8, the emission enhancement of DAP-1 shows almost no change compared with that of pH 7.4. The results suggest that DAP-1 can respond to Cys rapidly. Based on the above experimental results, we selected this optimal reaction time for the subsequent fluorescence measurements.

3.4. The sensitivity studies

On the basis of the above experiments, we also conduct concentration-dependent experiments to assess the sensitivity of DAP-1 (10 μM) toward Cys. As we can see from Fig. 5, DAP-1 alone in 10 mM PBS buffer solution (H_2O/DMSO = 99:1, pH 7.4) are almost no fluorescence. It is understandable that the fluorescence of DAP-1 was efficiently quenched by the acrylate group. However, the fluorescence intensity at 495 nm increased gradually with the increase of cysteine concentration. The fluorescence intensity was maximized when 10 equiv. Cys was added and the enhancement was up to 65-fold, indicating that Cys could effectively eliminate the acrylic ester moiety in DAP-1 to offer the chromophore compound 2. Moreover, there is a good linear relationship ($y = 8.18521\ x + 1.93607$, $R^2 = 0.9916$) between the fluorescence intensity at 495 nm (Fig. 6) and the concentrations of Cys (0–30 μM). The limit of detection was calculated to be 0.03 μM. Moreover, the curve in Fig. S9 shows a good linear relationship ($R^2 = 0.99479$) of fluorescence intensity versus the concentration of compound 2 (0–10 μM). The above results show that DAP-1 can well be applied for quantitative detection of Cys with high sensitivity.

3.5. The selectivity and competition studies

After we obtained the optimal solvent ratio and reaction time, the selectivity of DAP-1 (10 μM) to various amino acids were examined. As shown in Fig. 7, the fluorescence intensity increased rapidly at 495 nm when 10 equiv. Cys was added to the solution of DAP-1. However, the GSH and Hcy cause only slight fluorescence enhancement under the same conditions. Morever, the fluorescence intensity was negligible in the presence of other amino acids (Glu, Thr, Ser, Ala, Asp, Phe, Val, Leu, His, Trp, IIe, Arg, Lys). These results indicated that DAP-1 could selectively distinguish Cys from GSH and Hcy. It is understandable that the Michael addition/cyclization between acrylic ester and Cys generally exhibited faster reaction kinetics than GSH and Hcy [12,58–60]. Importantly, DAP-1 has two acrylate groups, which could make the distinction of the reaction kinetics with biothiols even more evident. Another reason for this result could be the effect of pKa. It is kown that the pKa values of Cys, Hcy and GSH are 8.30, 8.87 and 9.20, respectively [61], the Cys pKa is relatively lower. Under our test condition (pH = 7.4), the thiol in Cys was more likely to be converted to thiolate, which is a better nucleophile in conjugate addition, thus offering DAP-1 to actualize high selectivity for Cys over GSH and Hcy. Moreover, competitive experiments were also implemented to illustrate DAP-1 can still keep its sensing response toward Cys without interference by other amino acids (Fig. 8). As is shown in Fig. 8, the Cys can well be detected even in the presence of other amino acids and there is no adverse interference from these amino acids. The results indicate that DAP-1 could selectively distinguish Cys from GSH and Hcy.

3.6. Proposed mechanism of DAP-1 with Cys

The reaction between acrylate group and biothiols has been well studied by Strongin et al [12,62]. According to these literatures and our experiment results, proposed detection mechanism of DAP-1 to Cys was shown in Scheme 3A. The reaction first involved a conjugate addition of Cys to α,β-unsaturated carbonyl group of DAP-1 to generate the corresponding thioether (3), a transient intermediate, which could subsequently undergo an intramolecular cyclization to afford the chomophore compound 2. The high selectivity of DAP-1 for Cys over GSH and Hcy could be illustrated by the fact that Cys exhibits faster kinetics than GSH and Hcy in the process of intramolecular intramolecular cyclization between acrylate groups and biothiols, owing to the more kinetically favorable formation of a seven-membered ring product (2a, n = 1). Particularly, DAP-1 has double acrylate groups, which could make the distinction of reaction kinetics between these biothiols even more evident. To confirm the above mechanism, the product was separated after DAP-1 reacted with Cys and HR-MS analysis was displayed. As shown in Fig. S6, The peaks of DAP-1 (*m/z* 255.0784) and compound 2 (*m/z* 363.1003) could be observed. ^{1}H NMR spectra of DAP-1, DAP-1-Cys reaction products and compound 2 were examined to further verify this mechanism. As shown in Scheme 3B, after reacting with Cys, the characteristic proton signals of the two acrylate groups of DAP-1 at 6.60, 6.47, 6.31, 6.21 and 6.10 ppm disappear and two new peaks at 10.31 and 14.26 ppm corresponding to Phenolic hydroxyl groups are distinctly observed, which were consistent with that of compound 2, demonstrating that the reaction from Cys was compound 2. Moreover, the structure of the cleaved cyclisation product 2a was proved by 1H NMR spectrum (Fig. S11). The above results supported the proposed reaction mechanism between DAP-1 and Cys.

3.7. Effects of pH

Appropriate pH condition for successful operation of the fluorescence detecting was studied. As show in Fig. 9, the fluorescent intensity of DAP-1 (10 μM) was not changed in the pH range of 4–10, indicating that DAP-1 could maintain good stability in a relatively wide pH range. When DAP-1 was treated with 10 equiv. Cys, obvious fluorescent enhancement could be observed within the pH range from 7.5 to 8.5. The results demonstrated that DAP-1 could be applied in the detection of Cys in physiological circumstances. However, at pH above 8.5, the fluorescence intensity decreased, the reason may be due to the deprotonation of the thiol moieties.

3.8. Fluorescence imaging and cytotoxicity assay

To evaluate the practical utility of DAP-1 (10 μM) for selectively fluorescent imaging of Cys in living cells, cell-based experiments were performed (Fig. 10). Initially, the living HeLa cells showed almost no background fluorescence in the absence of DAP-1 (Fig. 10A). However, strong green fluorescence could be observed when HeLa cells were treated with probe DAP-1 (Fig. 10B). The green fluorescence was stronger when exogenous Cys (100 μM) was added (Fig. 10C). These results indicate that DAP-1 can permeate into HeLa cells and react with endogenous Cys to yield green fluorescence. As a control experiment, when HeLa cells were incubated with NEM (1 mM, a thiol-blocking

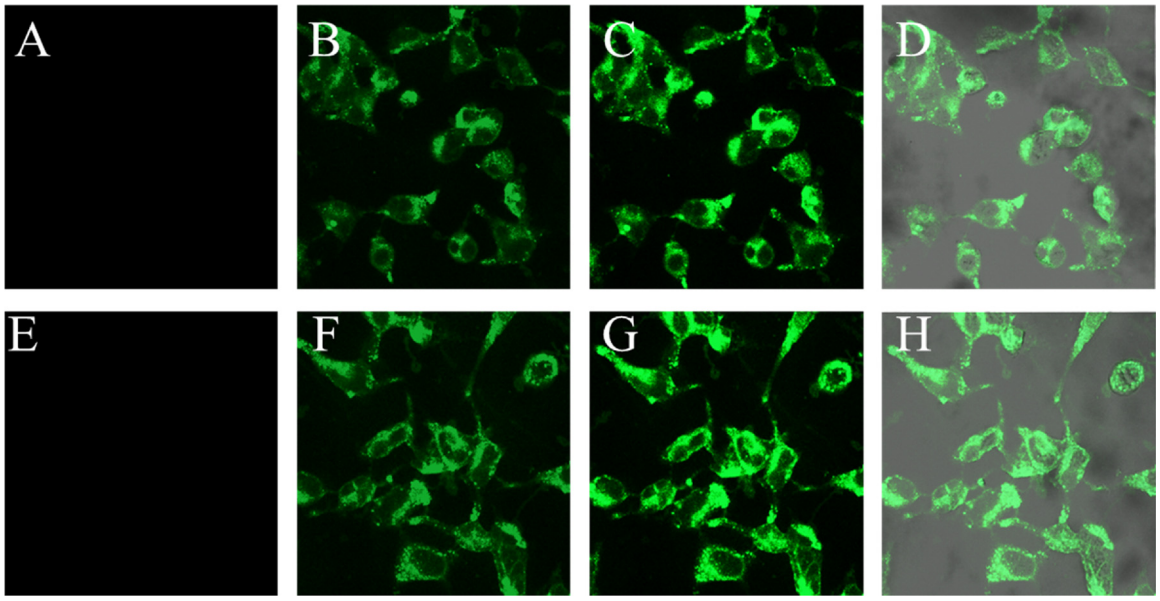

Fig. 10. (A) Confocal fluorescence microscope image of HeLa cells only, (B) images of cells + DAP-1 (10 μM), (C) images of cells + DAP-1 (10 μM) + Cys (100 μM), (D) the overlay image of C and its Bright-field image (E) images of cells + NEM (1 mM) + DAP-1 (10 μM), (F) images of cells + NEM (1 mM) + Cys (100 μM) + DAP-1 (10 μM), (G) images of cells + NEM (1 mM) + excess Cys + DAP-1 (10 μM), (H) the overlay image of G and its Bright-field image. Scale bar = 20 μm, E_{ex} = 405 nm.

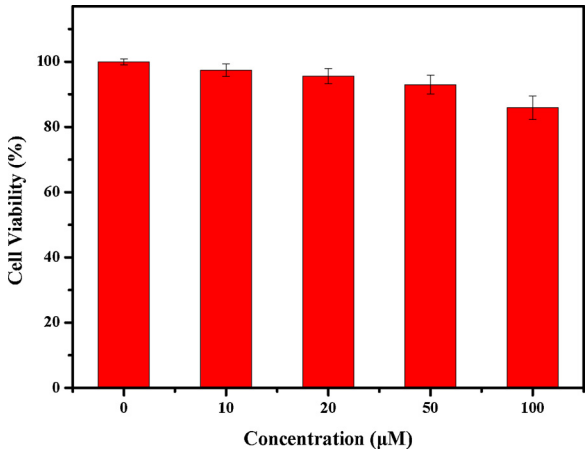

Fig. 11. Cell viability was quantified by the MTT assay (HeLa cells, 24 h).

reagent) and then treated with DAP-1 (10 μM), no fluorescence could be observed (Fig. 10E), suggesting that intramolecular Cys has been completely removed by NEM. However, when cells were incubated with NEM (1 mM) and then treated with Cys (100 μM) and DAP-1, the cells showed green fluorescence again (Fig. 10F) and the green fluorescence was stronger when excess Cys was added (Fig. 10G). Moreover, the overlay image (Fig. 10D, 10 H) of confocal fluorescence and bright-field images demonstrated that the fluorescence was obvious. These results implied that DAP-1 was membrane-permeable and could detect Cys in living cells. Conventionally, a cell viability assay was performed to assess the cytotoxicity of DAP-1. Different concentration of DAP-1 (0, 10, 20, 50 and 100 μM) was added to the HeLa cells (Fig. 11). The results showed that cells could still keep a high viability (near 86%) even with 100 μM DAP-1 at 37 °C for 24 h and no significant difference was observed between the groups, suggesting the great potential of DAP-1 in terms of its low cytotoxicity.

4. Conclusions

In conclusion, we introduce two acrylate groups into a HPQ derivative to develop a double acrylate-functionalized fluorescent probe DAP-1. DAP-1 displays a large Stokes shift (162 nm). The addition of Cys to DAP-1 solution would result in a strong fluorescence enhancement due to conjugated addition/cyclization sequence mechanism. Besides, DAP-1 displays excellent selectivity and sensitivity for Cys over Hcy and GSH. The fluorescence titration results revealed that the response time of DAP-1 to Cys could be accomplished within 15 min and the limit of detection was calculated to be as low as 0.03 μM. Importantly, DAP-1 was membrane-permeable and could detect Cys in living cells.

Acknowledgements

This work was financially supported by National Natural Science Foundation of China (NO. 31471693), Jiangsu Provincial Policy Guidance Plan (university-industry-research cooperation) prospective joint research projects (BY2016005-07) and Jiangsu Agricultural Science and Technology Innovation Fund (CX(17)3052). We thank the editors and the anonymous reviewers.

Appendix A. Supplementary data

Supplementary material related to this article can be found, in the online version, at doi:https://doi.org/10.1016/j.jphotochem.2018.07.014.

References

[1] K.G. Reddie, K.S. Carroll, Expanding the functional diversity of proteins through cysteine oxidation, Curr. Opin. Chem. Biol. 12 (2008) 746–754.
[2] S.Y. Zhang, C.N. Ong, H. Shen, Critical roles of intracellular thiols and calcium in parthenolide-induced apoptosis in human colorectal cancer cells, Cancer Lett. 208 (2004) 143–153.
[3] Z.A. Wood, E. Schröder, J.R. Harris, L.B. Poole, Structure, mechanism and regulation of peroxiredoxins, Trends Biochem. Sci. 28 (2003) 32–40.
[4] H.S. Jung, J.H. Han, T. Pradhan, S. Kim, S.W. Lee, J.L. Sessler, S.W. Lee, T.W. Kim, C. Kang, J.S. Kim, A cysteine-selective fluorescent probe for the cellular detection of cysteine, Biomaterials 33 (2012) 945–953.
[5] H.J. Forman, H.Q. Zhang, A. Rinna, Glutathione: overview of its protective roles, measurement, and biosynthesis, Mol. Asp. Med. 30 (2009) 1–12.
[6] A.R. Rosa, N. Singh, E. Whitaker, M. deBrito, A.M. Lewis, E. Vieta, G.C. Churchill, J.R. Geddes, G.M. Goodwn, Altered plasma glutathione levels in bipolar disorder indicates higher oxidative stress; a possible risk factor for illness onset despite

normal brain-derived neurotrophic factor (BDNF) levels, Psychol. Med. (Paris) 44 (2014) 2409–2418.
[7] G.L. Ellman, Tissue sulfhydryl groups, Arch. Biochem. Biophys. 1 (1959) 70–77.
[8] T. Inoue, J.R. Kirchhoff, Electrochemical detection of thiols with a coenzyme pyrroloquinoline quinone modified electrode, Anal. Chem. 72 (2000) 5755–5760.
[9] S.X. Feng, X.A. Li, Q.J. Ma, B.B. Liang, Z.Y. Ma, A highly selective and sensitive fluorescent probe for thiols based on a benzothiazole derivative, Anal. Methods 8 (2016) 6832–6839.
[10] T. Liu, F.J. Huo, J.F. Li, J.B. Chao, Y.B. Zhang, C.X. Yin, An off-on fluorescent probe for specifically detecting cysteine and its application in bioimaging, Sensor. Actuators B: Chem. 237 (2016) 127–132.
[11] B.K. Rani, S.A. John, A novel pyrene based fluorescent probe for selective detection of cysteine in presence of other bio-thiols in living cells, Biosens. Bioelectron. 83 (2016) 237–242.
[12] X.F. Yang, Y.X. Guo, R.M. Strongin, Conjugate addition/cyclization sequence enables selective and simultaneous fluorescence detection of cysteine and homocysteine, Angew. Chem. Int. Ed. 50 (2011) 10690–10693.
[13] W.H. Wang, K. Vellaisamy, G.D. Li, C. Wu, C.N. Ko, C.H. Leung, D.L. Ma, Development of a long-lived luminescence probe for visualizing β-galactosidase in ovarian carcinoma cells, Anal. Chem. 89 (2017) 11679–11684.
[14] C.Y. Li, M.X. Yu, Y. Sun, Y.Q. Wu, C.H. Huang, F.Y. Li, A nonemissive iridium(III) complex that specifically lights-up the nuclei of living cells, J. Am. Chem. Soc. 133 (2011) 11231–11239.
[15] M. Walter, C. Chaban, K. Schütze, O. Batistic, K. Weckermann, C. Näke, D. Blazevic, C. Grefen, K. Schumacher, C. Oecking, K. Harter, J. Kudla, Visualization of protein interactions in living plant cells using bimolecular fluorescence complementation, Plant J. 40 (2004) 428–438.
[16] C.D. Chen, S.Y. Oh, J.D. Hinman, C.R. Abraham, Visualization of APP dimerization and APP-Notch2 heterodimerization in living cells using bimolecular fluorescence complementation, J. Neurochem. 97 (2006) 30–43.
[17] J.B. Liu, L.J. Liu, Z.Z. Dong, G.J. Yang, C.H. Leung, D.L. Ma, An aldol reaction-based iridium(III) chemosensor for the visualization of proline in living, Cells, Sci. Rep. 6 (2016) 36509.
[18] M. Rafii, R. Elango, G. Courtney-Martin, J.D. House, L. Fisher, P.B. Pencharz, High-throughput and simultaneous measurement of homocysteine and cysteine in human plasma and urine by liquid chromatography–electrospray tandem mass spectrometry, Anal. Biochem. 371 (2007) 71–81.
[19] D. Maheshwaran, S. Priyanga, R. Mayilmurugan, Copper (II)-benzimidazole complexes as efficient fluorescent probes for L-cysteine in water, Dalton Trans. 46 (2017) 11408-11407.
[20] K.S. Lee, J.M. Park, H.J. Park, Y.K. Chung, S.B. Park, H.J. Kim, I.S. Shin, J.I. Hong, Regenerative fluorescence "turn-on" probe for biothiols through Cu(II)/Cu(I) redox conversion, Sens.Actuators B: Chem. 237 (2016) 256–261.
[21] D.B. Chao, Y.X. Zhang, Aggregation enhanced luminescent detection of homocysteine in water with terpyridine-based Cu^{2+} complexes, Sens. Actuators B: Chem. 245 (2017) 146–155.
[22] H.S. Jung, J.H. Han, Y. Habata, C. Kang, J.S. Kim, An iminocoumarin-Cu(II) ensemble-based chemodosimeter toward thiols, Chem. Commun. (Camb.) 47 (2011) 5142–5147.
[23] Q. Wang, H. Wang, J. Huang, N. Li, Y. Gu, P. Wang, Novel NIR fluorescent probe with dual models for sensitively and selectively monitoring and imaging Cys in living cells and mice, Sens. Actuators B: Chem. 253 (2017) 400–406.
[24] P. Wang, Q. Wang, J. Huang, N. Li, Y. Gu, A dual-site fluorescent probe for direct and highly selective detection of cysteine and its application in living cells, Biosens. Bioelectron. 92 (2017) 583–588.
[25] M.M. Hu, J.L. Fan, H.L. Li, K.D. Song, S. Wang, G.H. Cheng, X.J. Peng, Fluorescent chemodosimeter for Cys/Hcy with a large absorption shift and imaging in living cells, Org. Biomol. Chem. 9 (2011) 980–983.
[26] X.W. Cao, W.Y. Cao, W.Y. Lin, Q.X. Yu, A ratiometric fluorescent probe for thiols based on a tetrakis(4-hydroxyphenyl)porphyrin–Coumarin scaffold, J. Org. Chem. 76 (2011) 7423–7430.
[27] R. Chand, S.K. Jha, K. Islam, D. Han, I.S. Shin, Y.S. Kim, Analytical detection of biological thiols in a microchip capillary channel, Biosens. Bioelectron. 40 (2013) 362–367.
[28] Z.Y. Chen, Q. Sun, Y.H. Yao, X.X. Fan, W.B. Zhang, J.H. Qian, Highly sensitive detection of cysteine over glutathione and homo-cysteine: new insight into the Michael addition of mercapto group to maleimide, Biosens. Bioelectron. 91 (2017) 553–559.
[29] Y.J. Wang, Z.R. Liu, G.M. Ren, X.Q. Kong, W.Y. Lin, A fast-response two-photon fluorescent probe for the detection of Cys over GSH/Hcy with a large turn-on signal and its application in living tissues, J. Mater. Chem. B Mater. Biol. Med. 5 (2017) 134–138.
[30] X. Dai, Q.H. Wu, P.C. Wang, J. Tian, Y. Xu, S.Q. Wang, J.Y. Miao, B.X. Zhao, A simple and effective coumarin-based fluorescent probe for cysteine, Biosens. Bioelectron. 59 (2014) 35–39.
[31] X.J. Liu, D.L. Yang, W.Q. Chen, L. Yang, F.P. Qi, X.Z. Song, A red-emitting fluorescent probe for specific detection of cysteine over homocysteine and glutathione with a large Stokes shift, Sens. Actuators B: Chem. 234 (2016) 27–33.
[32] Z.H. Fu, X. Han, Y.L. Shao, J.G. Fang, Z.H. Zhang, Y.W. Wang, Y. Peng, Fluorescein-based chromogenic and ratiometric fluorescence probe for highly selective detection of cysteine and its application in Bioimaging, Anal. Chem. 89 (2017) 1937–1944.
[33] M. Gao, S.W. Li, Y.H. Lin, Y. Geng, X. Ling, L.C. Wang, A.J. Qin, B.Z. Tang, Fluorescent light-up detection of amine vapors based on aggregation-induced emission, ACS Sens. 1 (2016) 179–184.
[34] W. Liu, S.J. Liu, Y.Q. Kuang, F.Y. Luo, J.H. Jiang, Developing activity localization fluorescence peptide probe using thiol-ene click reaction for spatially resolved imaging of Caspase-8 in live cells, Anal. Chem. 88 (2016) 7867–7872.
[35] Z.Q. Guo, S.W. Nam, S.S. Park, J.Y. Yoon, A highly selective ratiometric near-infrared fluorescent cyanine sensor for cysteine with remarkable shift and its application in bioimaging, Chem. Sci. 3 (2012) 2760–2765.
[36] J.J. Zhang, J.X. Wang, J.T. Liu, L.L. Ning, X.Y. Zhu, B.F. Yu, X.Y. Liu, X.J. Yao, H.X. Zhang, Near-infrared and naked-eye fluorescence probe for direct and highly selective detection of cysteine and its application in living cells, Anal. Chem. 87 (2015) 4856–4863.
[37] H.Y. Zhang, W. Feng, G. Feng, A simple and readily available fluorescent turn-on probe for cysteine detection and bioimaging in living cells, Dyes Pigm. 139 (2017) 73–78.
[38] S.H. Xue, S.S. Ding, Q.S. Zhai, H.Y. Zhang, G.Q. Feng, A readily available colorimetric and near-infrared fluorescent turn-on probe for rapid and selective detection of cysteine in living cells, Biosens. Bioelectron. 68 (2015) 316–321.
[39] J.M. Shi, Y.J. Wang, X.L. Tang, W. Liu, H. Jiang, W. Dou, W.S. Liu, A colorimetric and fluorescent probe for thiols based on 1,8-naphthalimide and its application for bioimaging, Dyes Pigm. 100 (2014) 255–260.
[40] J. Mei, N.L.C. Leung, R.T.K. Kwok, J.W.Y. Lam, B.Z. Tang, Aggregation-induced emission: together we shine, united we soar!, Chem. Rev. 115 (2015) 11718–11940.
[41] Y. Hong, J.W.Y. Lam, B.Z. Tang, Aggregation-induced emission: phenomenon, mechanism and applications, Chem. Commun. (Camb.) 45 (2009) 4332–4353.
[42] Y.N. Hong, J.Y. Lam, B.Z. Tang, Aggregation-induced emission, Chem. Soc. Rev. 40 (2011) 5361–5388.
[43] Y.N. Hong, J.W.Y. Lam, B.Z. Tang, Aggregation-induced emission: phenomenon, mechanism and applications, Chem. Commun. (Camb.) 0 (2009) 4332–4353.
[44] X.G. Gu, G.X. Zhang, Z. Wang, W.W. Liu, L. Xiao, D.Q. Zhang, A new fluorometric turn-on assay for alkaline phosphatase and inhibitor screening based on aggregation and deaggregation of tetraphenylethylene molecules, Analyst 138 (2013) 2427–2431.
[45] J. Shi, S. Zhang, M.M. Zheng, Q.C. Deng, C. Zheng, J. Li, F.H. Huang, A novel fluorometric turn-on assay for lipase activity based on an aggregation-induced emission (AIE) luminogen, Sens. Actuators B: Chem. 238 (2017) 765–771.
[46] M. Gao, Q.L. Hu, G.X. Feng, B.Z. Tang, B. Liu, A fluorescent light-up probe with "AIE + ESIPT" characteristics for specific detection of lysosomal esterase, J. Mater. Chem. B Mater. Biol. Med. 2 (2014) 3438–3442.
[47] L.J. Tang, S.L. Ding, X.R. Zhang, K.L. Zhong, S.H. Hou, Y.J. Bian, A 2-(2′-hydroxyphenyl)quinazolin-4(3H)-one derived fluorescence 'turn on' probe for recognition of Hg^{2+} in water solution and its live cell imaging, J. Photochem. Photobiol. A Chem. 340 (2017) 15–20.
[48] L.J. Tang, S.L. Ding, X.M. Yan, A 2-(2′-hydroxyphenyl)quinazolin-4(3H)-one derived enaminone for fluorescence detection of Pd^{2+}, Inorg. Chem. Commun. 74 (2016) 35–38.
[49] L. Peng, S.D. Xu, X.K. Zheng, X.M. Cheng, R.Y. Zhang, J. Liu, B. Liu, A.J. Tong, Rational design of a red-emissive fluorophore with AIE and ESIPT characteristics and its application in light-up sensing of esterase, Anal. Chem. 89 (2017) 3162–3168.
[50] R.J. Li, L.Q. Yan, Z.W. Wang, Z.J. Qi, An aggregation-induced emissive NIR luminescent based on ESIPT and TICT mechanisms and its application to the detection of Cys, J. Mol. Struct. 1136 (2017) 1–6.
[51] X.J. Peng, F.L. Song, E. Lu, Y.N. Wang, W. Zhou, J.L. Fan, Y.L. Gao, Heptamethine cyanine dyes with a large stokes shift and strong fluorescence: a paradigm for excited-state intramolecular charge transfer, J. Am. Chem. Soc. 12 (2005) 4170–4171.
[52] W.Y. Feng, M.X. Li, Y. Sun, G.Q. Feng, Near-infrared fluorescent turn-on probe with a remarkable large stokes shift for imaging selenocysteine in living cells and animals, Anal. Chem. 11 (2017) 6106–6112.
[53] S. Chen, H. Li, P. Hou, A large stokes shift fluorescent probe for sensing of thiophenols based on imidazo[1,5-α]pyridine in both aqueous medium and living cells, Anal. Chim. Acta 993 (2017) 63–70.
[54] S. Chen, H. Li, P. Hou, Imidazo[1,5-α]pyridine-derived fluorescent turn-on probe for cellular thiols imaging with a large Stokes shift, Tetrahedron Lett. 58 (2017) 2654–2657.
[55] S. Chen, H. Li, P. Hou, A novel imidazo[1,5-α]pyridine-based fluorescent probe with a large Stokes shift for imaging hydrogen sulfide, Sens. Actuators B: Chem. 256 (2018) 1086–1092.
[56] H.J. Lee, H.J. Kim, Fluorescein aldehyde with disulfide functionality as a fluorescence turn-on probe for cysteine and homocysteine in HEPES buffer, Org. Biomol. Chem. 11 (2013) 5012–5016.
[57] Y.K. Yue, F.J. Huo, P. Ning, Y.B. Zhang, J.B. Chao, X.M. Meng, C.X. Ying, Dual-site fluorescent probe for visualizing the metabolism of cys in living cells, J. Am. Chem. Soc. 139 (2017) 3181–3185.
[58] H.M. Lv, D.H. Yuan, W.P. Liu, Y. Chen, C.T. Au, S.F. Yin, A highly selective ESIPT-based fluorescent probe for cysteine sensing and its bioimaging application in living cells, Sens. Actuators B: Chem. 233 (2016) 173–179.
[59] Y.K. Yue, C.X. Yin, F.J. Huo, J.B. Chao, Y.B. Zhang, Thiol-chromene click chemistry: A turn-on fluorescent probe for specific detection of cysteine and its application in bioimaging, Sens. Actuators B: Chem. 223 (2016) 496–500.
[60] W.Q. Chen, H.C. Luo, X.J. Liu, F.P. Qi, D.L. Yang, X.Z. Song, A fluorescent probe emitting in near-infrared region for sensitive and selective detection of biothiols in both solution and living cells, Tetrahedron Lett. 56 (2015) 7176–7179.
[61] M. Iciek, G. Chwatko, E. Lorenc-Koci, E. Bald, L. Wloderk, Plasma levels of total, free and protein bound thiols as well as sulfane sulfur in different age groups of rats, Acta Biochim. Polon. 51 (2014) 815–824.
[62] X.F. Yang, Y.X. Guo, R.M. Strongin, A seminaphthofluorescein-based fluorescent chemodosimeter for the highly selective detection of cysteine, Org. Biomol. Chem. 10 (2012) 2739–2741.